

## Numerical Analysis and Investigation of Aluminum Alloys in Electromagnetic Metal Forming Process

Kiran S.Bhole<sup>1</sup>, B.S.Kale<sup>2</sup>, P.D.Deshmukh<sup>3</sup> O.G.Sonare<sup>4</sup>

<sup>1,2,3,4</sup>Datta Meghe College of Engineering, Department of Mechanical Engineering, Airoli, Navi Mumbai, India  
Email:<sup>1</sup> kirandipali@gmail.com <sup>2</sup> bhrt\_kale@yahoo.co.in

**Abstract**— This paper deals with computer-aided analysis of Electromagnetic (EM) forming process based on simulation results of low speed versus high speed forming numerical model. Electromagnetic forming process consists of a die, electric coil, capacitor bank, transformer and diodes. A numerical method for modeling the high rate deformation and impact that occurs during the electromagnetic forming process is presented. The transient forming is done using FEM software packages to analyze the model. The body forces generated by electromagnetic induction are then used as the loading condition to model the high rate deformation of the work piece using an explicit dynamic finite element code. The analysis focuses on stress and strain generation between tool and sheet interaction, failure and buckling criterion to improve the formability and reduce the failure.

**Index Terms** — Forming, High velocity, Electromagnetic, forming, Aluminum.

### I. INTRODUCTION

EM forming process utilizes the energy of the magnetic field to deform the metal [1-11]. The capacitor bank is discharged across the forming coil through the discharge circuit. This causes a rapidly changing current, say  $I_1(t)$  to flow through the forming coil. This current has a transient magnetic field associated with it. The transient magnetic field induces a current, say  $I_2(t)$  in the workpiece. By Lenz's law, the direction of  $I_2(t)$  is such that it opposes the magnetic field that produced it. In other words,  $I_2(t)$  is opposite in direction to  $I_1(t)$ . Lorentz force acts between the two current carrying conductors. Since the currents are opposing, a repulsive force is developed between the coil and the workpiece. When this magnetic pressure exerted by the coil on the workpiece exceeds the yield stress of the workpiece material, the workpiece is thrown away from the coil i.e. it plastically deforms and expands.

Reference [12-14] outlined three different mechanisms that may account for increased formability: (i) the material constitutive behaviour changes at high-strain rates, leading to an increase in the rate of strain hardening and/or rate sensitivity; (ii) it may be possible that inertial effects promote more diffuse neck

development, hence leading to higher ductility; and (iii) the impact with the die wall at high velocity causes the material to plastically spread radially in a process that may be thought of as "inertial ironing". Reference [15] examined the effect of tool/sheet interaction on damage evolution in EM forming through free-form and conical dies experiments using 1mm ALU5754MF sheet. In that study, they utilized a damage-based material model to demonstrate that the tool/sheet interaction had a significant effect in suppressing necking and damage evolution.

Reference [16] made one of the earliest attempts to develop an analytical method by which EM forming may be investigated through establishing basic equations that describe the physical phenomena.

The role of "hyperplasticity" in sheet-metal applications through the acquisition of basic material formability data and the dynamics of the high-velocity impact of the sheet and die are also assessed. The three-dimensional finite-element modeling capability developed in this work is used to model conical cavity which are driven by an EM coil.

### II. EM-FORMING PARAMETERS

#### A. Tooling Details

Cavity corresponds to the dimensions as shown in Fig. (2). The die cavity is of diameter 106 mm, with an entry radius of 10 mm. Cavity height is taken variable as 30 mm, 33 mm, 36 mm. A flat spiral pancake coil Fig. (1) is considered that locates the "dead spot" (region of low magnetic pressure) that occurs at the center of the winding of a spiral coil. The coil is wound from copper wire with a gauge of 10.

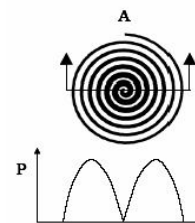


Fig. 1. Pressure distribution along section of pancake coil

### B. Electrical Parameters for EM-forming System

Table 1 summarizes the relevant EM Forming parameters and their values for the numerical results described herein. The energy levels used in the simulations range from 4 kJ to 6.25 kJ, with a current-discharge frequency 44.721 kHz.

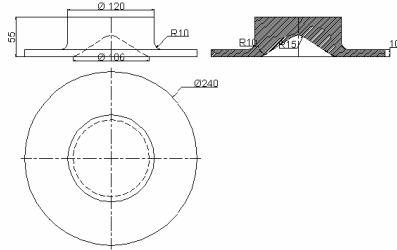


Fig. 2. EM-forming die for numerical simulation.

Table 1 EM forming quantities taken for numerical solution

EM forming parameters	Values
Charge voltage	4 – 5 KV
System capacitance	500µF
Total system inductance	1 µH
Energy levels	4 – 6.25 kJ
Frequency	44.721kHz
Coil resistivity	$1.7e^{-8} \Omega / m$
Aluminum resistivity	$2.77e^{-8} \Omega / m$
Air gap	4mm
Peak-current range	89.44 – 111.803 KA

### C. Materials

The materials considered are two types of aluminium alloy sheet which are ALU5754MF and ALU5182MF of thickness 1 mm and 1.5 mm. The material properties measured along the rolling direction are presented in Table 2. These materials were investigated, since they are candidates for automotive structural applications. ALU5182MF is about 25% stronger than ALU5754MF, allowing examination of any strength effect in the numerical simulation, while the two-sheet thickness values allows this parameter to be investigated as well.

Table 2 Material properties for the samples

Material	Yield Strength (MPa)	Ultimate Tensile Strength (MPa)	Poisson's ratio
ALU5754MF	123	224	0.22
ALU5182MF	133	281	0.29

### III. NUMERICAL MODELLING

Numerical modeling of the electromagnetic-forming process requires the simultaneous solution of the electromagnetic, structural and thermal equations. In the current modeling efforts, thermal-conduction effects were neglected, since the process was assumed to be adiabatic.

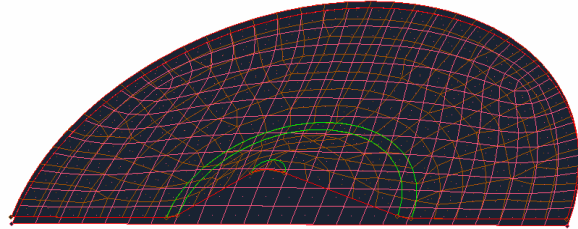


Fig. 3. Finite -element mesh of half section die and sheet

The introduction of thermal-conduction effects into the numerical model is left for future work, once the physics due to the electromagnetic and structural phenomena is better understood. In order to simulate the structural behaviour in EM forming, Altair HyperWorks 6.0 (HyperMesh, HyperForm, HyperView), LS-DYNA, an explicit dynamic finite element Program is used.

The exploded view of the finite-element mesh used to model the EM-forming system is shown in Fig.(3). The mesh is used for structural domains. The rigid tooling surfaces are considered in the structural calculation. For simplicity, the coil and die are treated as rigid bodies, while the workpiece is modeled with deformable brick elements. An isotropic, linear plasticity model is adopted for the workpiece. The electromagnetic pressures Eq.(1) [1] are applied at each node of the workpiece.

$$P_r = \frac{\mu_0 I^2 N^2}{2\pi^2} \left\{ \tan^{-1} \left[ \frac{-2gr}{g^2 + a_2^2 - r^2} \right] + \tan^{-1} \left[ \frac{-2gr}{g^2 + a_1^2 - r^2} \right] \right\} \quad \text{Eq.(1)}$$

where  $I$  = current in Amperes,  $N$ = number of turns in coil,  $g$  = distance from the coil to the workpiece in meters,  $a_1$  = distance from the center of the coil to the first wind of the coil in meters,  $a_2$  = distance from the center of the coil to the last wind of the coil in meters and  $r$  = radius in meters. Pressure calculated according to Eq.(1) is peak value at radial distance 'r' from centre. According to first order analysis of EM forming process the pressure at each such point also varies with respect to time given by Eq.(2).

$$P_r = P_{rmax} e^{-\alpha} \sin(\omega t) \quad \text{Eq.(2)}$$

where exponential decay term ,  $\alpha$ , can be expressed as

$$\alpha = \frac{R}{2L} \quad \text{Eq.(3)}$$

where R= resistivity of sheet and L = inductance of total system.

The velocity of sheet can be calculated by Eq. (4),

$$\text{Velocity, } v = \frac{E}{\int Pr 2\pi r dr} \quad \text{Eq.(4)}$$

where E = Rate of energy released.

For simplicity of design pressure distribution over the sheet may be assumed uniform over the sheet.

#### IV. NUMERICAL RESULTS

Successive iterations were performed at increasing energy levels until the energy level associated with the “point of failure” was established. After this, samples were formed at two or three lower energy levels and one at a higher level. This sequence provides information about the extent of deformation-strain and thinning history in the samples leading up to the point of failure. The depth and geometry of the die cavity was also varied.

Results of the entire cone insert cavity fill simulations performed and summarizes the process conditions are listed in Table 3. Failure in the cone occurs along the point of tangency between the sheet and cone surface. The failure in this location is due to thinning and necking at the tangency point between the sheet and die due to frictional forces at the die. As main mode of deformation in the failure zone is plane strain. The strains decrease as one moves from the failure site towards the edge of the die. The average cavity height for 1mm ALU5754MF was 24.3 mm [12] compared to almost 38 mm for the “safe” EM sample. In conventional forming, the friction between the punch and workpiece leads to non-uniform strain distributions. The distributed body forces in EM-forming eliminate frictional contact and promote comparatively uniform major strain distributions and very good cone heights.

Table 3. Summary of Numerical simulations carried with 7 turn pancake coil and 500 $\mu$ F capacitor bank.

Material	Thickness (mm)	Charge voltage (KV)	Peak current (KA)	Depth of cavity (mm)	Remark (Failure /Safe)
ALU5754MF	1	4.0	89.44	30	Safe
ALU5754MF	1	4.0	89.44	33	Safe
ALU5754MF	1	4.0	89.44	36	Safe
ALU5754MF	1	4.5	100.6	30	Failure
ALU5754MF	1	4.5	100.6	33	Safe

ALU5754MF	1	4.5	100.6	36	Safe
ALU5754MF	1	5.0	111.8	30	Failure
ALU5754MF	1	5.0	111.8	33	Failure
ALU5754MF	1	5.0	111.8	36	Safe
ALU5754MF	1.5	4.0	89.44	30	Failure
ALU5754MF	1.5	4.0	89.44	33	Safe
ALU5754MF	1.5	4.0	89.44	36	Failure
ALU5754MF	1.5	4.5	100.6	30	Safe
ALU5754MF	1.5	4.5	100.6	33	Safe
ALU5754MF	1.5	4.5	100.6	36	Failure
ALU5754MF	1.5	5.0	111.8	30	Failure
ALU5754MF	1.5	5.0	111.8	33	Safe
ALU5754MF	1.5	5.0	111.8	36	Safe
ALU5182MF	1	4.0	89.44	30	Safe
ALU5182MF	1	4.0	89.44	33	Failure
ALU5182MF	1	4.0	89.44	36	Failure
ALU5182MF	1	4.5	100.6	30	Safe
ALU5182MF	1	4.5	100.6	33	Safe
ALU5182MF	1	4.5	100.6	36	Failure
ALU5182MF	1	5.0	111.8	30	Failure
ALU5182MF	1	5.0	111.8	33	Failure
ALU5182MF	1	5.0	111.8	36	Safe
ALU5182MF	1.5	4.0	89.44	30	Failure
ALU5182MF	1.5	4.0	89.44	33	Failure
ALU5182MF	1.5	4.0	89.44	36	Failure
ALU5182MF	1.5	4.5	100.6	30	Failure
ALU5182MF	1.5	4.5	100.6	33	Safe
ALU5182MF	1.5	4.5	100.6	36	Safe
ALU5182MF	1.5	5.0	111.8	30	Failure
ALU5182MF	1.5	5.0	111.8	33	Safe
ALU5182MF	1.5	5.0	111.8	36	Failure

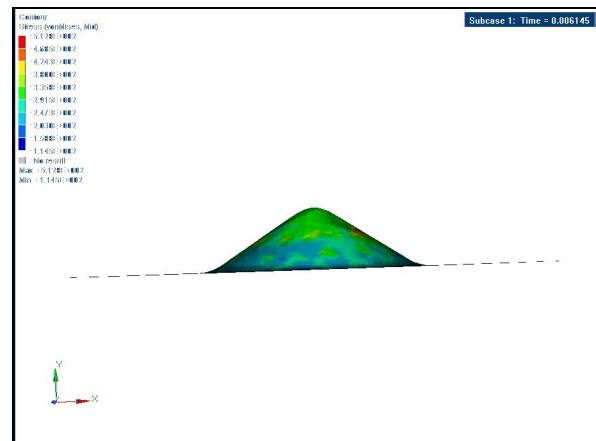


Fig. 4. Stress (VonMises) image

Figs.(4-5) shows images of stress (VonMises), and % thickness reduction obtained through simulation result on ALU5754MF 1 mm thick sheet carried with conventional low velocity 5 m/s respectively whereas Figs.(6-7) also shows images of stress (VonMises) and % thickness reduction obtained through simulation result on ALU5754MF 1mm thick sheet carried with typical high velocity of EM forming 100 m/s respectively.

From both set of results better control over thickness of deformed sheet with high velocity can be observed.

## V. NUMERICAL PREDICTIONS

High plastic strains occur in the regions of the workpiece that come into contact with the conical protrusion, with the highest strains at the tangency point of the sheet-tooling contact. The model predicts that the mode of deformation at the center of the dome is that of a biaxial stretching. Due to this biaxial stretching, thinning and necking also occurs at the centre point which leads to failure. It is also seen that as impact velocity increases deformation becomes more uniform but plastic strain reduces particularly at centre. The impact velocity between the workpiece and die in these models varies from 75 m/s to 150 m/s

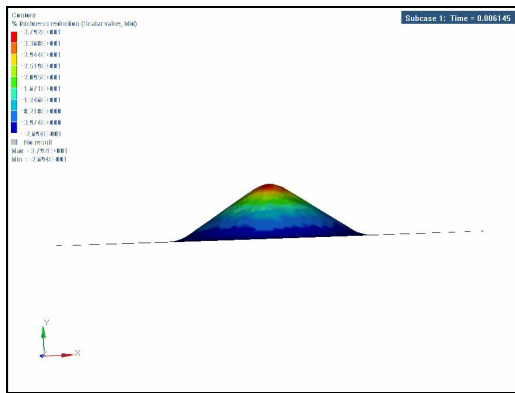


Fig. 5. Percentage thickness reduction image.

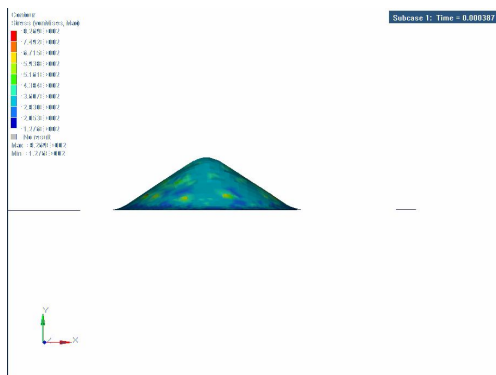


Fig. 6. Stress (VonMises) image

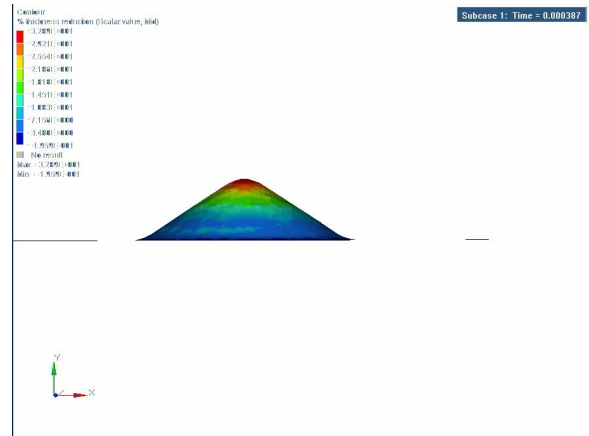


Fig. 7. Percentage thickness reduction image.

## .VI. DISCUSSION

The current series of simulation have served to illustrate the role of discharge voltage, alloy, sheet thickness, and die geometry on the EM-forming response of aluminium-alloy sheet. One improvement in the current die design that should be considered is to increase the die-entry radius in order to prevent tearing at this location. This modification may result in higher “safe strains”. A larger cavity size would also be beneficial. In the current simulations , the die entry radius was only 10mm, whereas conventional formability testing prescribes a much higher radius to minimize bending effects. The benefits of EM forming as a “punchless process” were manifested in very large cone heights compared to conventional values. In future, improved instrumentation to measure transient displacement and/or high-speed photography would considerably aid validation of these simulation models.

Consideration of Joule heat must also be added in future simulation efforts. Nonetheless, the current scheme provides a useful tool for predicting the response of sheet metal under EM-forming conditions and for future industrial process and die-design efforts.

## VII. CONCLUSION

The current simulations provide reasonable prediction of workpiece deformation and strain distribution. The models were able to predict the areas in workpiece that would experience thinning. Thus it can be concluded that EM forming is better forming process when compared to low speed forming process for aluminium alloys as superior cone heights and better control over thinning can be obtained through the elimination of punch-friction.

## ACKNOWLEDGEMENTS

Technical support for this study from Datta Meghe college of Engineering, Airoli is gratefully acknowledged.

### VIII. REFERENCES

- [1] J.Imbert Boyd, "Increased formability and the effects of tool/sheet interaction in Electromagnetic forming of Aluminium Alloy Sheet", Masters Thesis, University of Waterloo, Waterloo, Ontario, Canada,2005.
- [2] A.G. Mamalis, D.E. Manolakos, A.G. Kladas, A.K. Koumoutsos, "Physical principles of electromagnetic forming process: a constitutive finite element model", *Journal of Material Processing Technology* 161, pp. 294-299, 2005
- [3] Mala Seth, Vincent J. Vohnout, Daehn, "Formability of steel in high velocity impact", *Journal of Material Processing Technology* 168, pp.390-400, 2005
- [4] J.Mackerle, "Finite element analyses and simulations of sheet metal forming processes" *Engineering Computations Emerald Research Journal*, Vol.21, pp.891-940,2004
- [5] A. Giannoglou, A. Kladas, "Electromagnetic forming A coupled numerical Electromagnetic -mechanical-electrical approach to measurements", *Engineering Computations Emerald Research Journal* ,Vol.23, pp.789-799,2004.
- [6] A. Farschtschi, T.Richter, "Application of finite network theory to the transient process of Electromagnetic Forming", Progress in Electromagnetics Research Symposium, Cambridge, USA, March26-29, pp.465-469,(2006).142,pp.744-754, 2003.
- [7] Young-Bae, Heon-Young, Soo-Ik, "Design of axial/torque joint made by electromagnetic forming", *Thin-Walled Structures*,43,pp.826-844,2004.
- [8] Francois, Kay Hameyer, "Computation of electromagnetic force densities: Maxwell stress tensor vs. virtual work principle", *Journal of computational and applied mathematics*, 168, pp. 235-243,(2003)
- [9] G.K. Fenton, G.S. Daehn, "Modeling of electromagnetically formed sheet metal", *Journal of Material Processing Technology* 75, 6–16, 1998.
- [10] F.M.Song, X. Zhang, "A study of electromagnetic forming", *Journal of Material Processing Technology* 151, pp.372-375, 2004
- [11] I.V. Belyy, S.M. Fertik, L.T. Khimenko, "Electromagnetic Metal Forming Handbook", English version of Russian book translated by M.M. Altynova, *Department of Materials Science and Engineering, The Ohio State University*, 1996.
- [12] I.V. Belyy, S.M. Fertik, L.T. Khimenko, "Electromagnetic Metal Forming Handbook", English version of Russian book translated by M.M. Altynova, *Department of Materials Science and Engineering, The Ohio State University*, 1996.
- [13] V.S. Balanethiram, X. Hu, M. Altynova, G.S. Daehn, "Hyperplasticity: enhanced formability at high rates", *J. Mater. Process. Technol. (Neth.)* 45 (1–4) pp. 595–600, 1 September 1994.
- [14] Dong-Kyun Min, Dong-Won Kim, "A finite element analysis of electromagnetic tube compression process", *Journal of Material Processing Technology* 38, pp.29-40, 1993.
- [15] D.A.Oliveira, M.J. Worswick, M. Finn, D. Newman, "Electromagnetic Forming of aluminium alloy sheet: Free-form and cavity fill experiments and model", *Journal of Material Processing Technology* 170, pp.350-362, 2005.
- [16]Anter El-Azab, Mark Garnich, Ashish Kapoor, "Modeling of the electromagnetic forming of sheet metals: State –of –the art and future needs", *Journal of Material Processing Technology*142, pp.744-754, 2003.
- [17] Jablonski Winkler, "Analysis of the electromagnetic forming process", *Journal of Material Processing Technology*20, pp.315-325, (1977).